Journal of Himalayan Earth Sciences Volume 55, No. 1, 2022 pp. 40-49

Mineral chemistry of pyrite by EPMA mapping from the Senjedeh Gold deposit, Iran

Zahra Nourian Ramsheh[1], Seyedeh Narges Sadati[2*], Mohammad Yazdi[1], Jingwen Mao[3], and Fariborz Masoudi[1]

[1]Department of Geology, Faculty of Earth Science, Shahid Beheshti University, Tehran, Iran
[2]Department of Geology, Faculty of Science, University of Mohaghegh Ardabili, Ardabil, Iran
[3]MLR Key Laboratory of Metallogeny and Mineral Assessment, Institute of Mineral Resources, Chinese Academy of Geological Sciences, 100037 Beijing, China
**Corresponding author's email: Sadati_sn@uma.ac.ir*
Submitted date: 09/04/2021 Accepted date: 01/03/2022 Published online: 31/03/2022

Abstract

The Senjedeh gold deposit is situated 60 km southwest of Delijan in the central section of Sanandaj-Sirjan metamorphic belt. Most of rocks in this region have undergone greenschist to lower amphibolite metamorphism. The gold mineralization in the study area occurs as quartz sulfide veins in metarhyolite host rock. In order to detect the abundance of gold and associated elements in the pyrite using the techniques of mineralogical studies, electron probe microanalysis (EPMA) and back-scattered imaging through thin and polished sections in the Senjedeh gold deposit. Two generations of pyrite recognised: first generation, being anhedral to subhedral, (G1) are oriented along foliation contain high to medium gold content(up to 810ppm), shows deformed and fractured character. The second generation of pyrite (G2) is euhedral with medium to low gold content (below limit of detection up to 110ppm). According to electron back-scattered image and EPMA data, the presence of gold mainly occurs as submicroscopic-microscopic inclusions and invisible particles in microfractures of pyrite. Also based on EPMA mapping it is concluded that first-generation of pyrites contain high level of cobalt which could be a good indication of the presence of mafic and ultramafic rocks as a source of hydrothermal solutions compared to felsic rocks and consistent with orogenic gold deposit.

Keywords: Pyrite, EPMA, Senjedeh, Gold, Mineral chemistry

1. Introduction

The quartz vein-type gold deposits in the central part of Sannandaj-Sirjan metamorphic belt are obviously hosted by the metavolcanic (mostly green schist), and metasedimentary rocks and they are generally fractured controlled, faults and folds(Fig. 1and Fig. 2). The Gold- bearing pyrites in the Senjedeh deposit hosted in acidic volcanic rocks such as rhyolite and dacite which in some places affected by Argillic alteration. These rocks with mylonitic textures are widely exposed in the area.

Since 1950s, exploration studies have been extensively conducted in the Sannandaj- Sirjan metamorphic belt (e.g. Khoei 1987; Masoudy, 1997, Mohajjel et al., 2003, Alavi, 2004, Ghazban and Singer 2006). The mining activities involve excavations, predominantly in the form of tunnels, trenches and carvingsas observed in the old mines. In the last few decades, a large number of literature was produced on the geochemistry, tectonic, ore genesis and evolution in the region (e.g. Khoei 1987; Ghazban and Singer 2006; Agangiet al. 2015).

Pyrite is a major phase in the Gold-bearing deposits (Amponsah et al. 2016). So this mineral is the most important carriers of gold in the Senjedeh area in which gold exist as visible and invisible gold. If pyrite is precipitated directly from solution, its composition can provide important information on source of fluid and ore-forming processes(Agangi et al., 2015, Farhan et al., 2021). To date, no information has been provided on the composition of the pyrite in the Senjedeh deposit. Understanding geological conditions which could change pyrite composition is essential for using it as a tool for geochemical studies (Steven et al. 2013). In this paper, geochemical data obtained through electron probe microanalysis (EPMA) and electron

back-scattered images (BSE), are presented on a sample collected from the Senjedeh gold deposit, Muteh mining district to establish the different generations of pyrite and the distribution of gold in pyrite.

2. Geological setting

The Senjedeh gold deposit is located in the middle part of Sanandaj_ Sirjan zone. This zone is belonging to the Alpine-Himalayan orogenic and metallogenic belt (Alipour-Asll, 2018) (Fig. 1). This orogenic system is responsible for the formation of various gold ore types associated with detachment, subduction, collision and post-continental collision (Aliyari et al. 2012). The development of this zone linked to the opening of Neotethys at the end of the Paleozoic followed by continental collision between the Arabian and Eurasian plates at the late Cretaceous (Alavi 2004;Mohajjelet al. 2003; Almasiet al. 2017). Sanandaj- Sirjan metamorphic zone mainly contains Paleozoic to Cretaceous metamorphic rocks which are intruded by Jurassic to Eocene intrusive bodies (Fig. 1)(Masoudi 1997). Rock units exposed in the area consist of NW-SE trending deformed and metamorphosed volcano-sedimentary and acidic volcanic rocks of the Black Mountain(showing greenschist to lower amphibolite metamorphism) whose economic gold sections are located in three shear zones with normal faults and 3 to 6 m thickness(Fig. 1). (Abdolahi et al. 2009). These rocks involved crushed and heavily silicified gray metarhyolites in which gold is concentrated. The shear zones are separated from each other by sections of grayish brown metarhyolitic tailings, all these sections are part of the green schist complex (Fig. 2A-D).These units are characterized by several phases of intense deformation that lead to the generation of different fabrics and structures.

Structural studies carried out in the Mouteh area indicate its formation over several deformational stages that have caused folding and faulting in the area. The most prominent deformation phenomenon in the region is the N40W trend of young normal faulting that cuts metamorphisic fabrics. All alteration and mineralization zones are found along these faults. This is indicative of the genetic role of these faults in the Senjedeh mine and the entire Mouteh region. In fact, these faults act as conduits for ascending ore solutions, so the main alteration and ore formation in the Senjedeh mine is related to the N40W trend faulting. In the study area the host rock has been affected by different degrees of alteration. The hydrothermal alteration associated with the gold event in this area is accompanied by bleaching of the wall or host rock. This alteration exists symmetrically around the veins. The dominant alteration in the host rocks of Senjedeh Mine is often siliceous and occurs more often in veins and at sites of joint density. In addition, in some parts of the mine sericitic alteration, argillic (kaolinitic) alteration, pyritization, limonitization, as well as trace feldspar alteration (albite type) are also observed (Fig. 2B-D). In the ore sections, the alteration pattern is similar to the most of gold-bearing metamorphic belts(Goldfarb et al. 2005), so that sulfidization and siliceous alteration is developed in the inner parts of the ore zone, carbonate and sericitic alteration is found in the middle part and chlorite alteration in the outer part and all rock units in the area. Field and microscopic studies indicate the spatial and temporal relationship of hydrothermal alteration with deformation and mineralization, so that the location of severe alterations is maximal in areas where normal faults are observed (Fig 2. A-D). The argillic alteration extends more to the upper parts of the deposit and is likely related to the meteoritic waters (Fig. 2E).

The ore-bearing quartz veins are shortened and thickened in some places and generally cut foliation and metamorphic structures (Fig. 2F). This indicates the injection of hydrothermal fluids in the region and the formation of gold quartz veins coinciding with the active tectonics of the region which has led to the formation of budding quartz veins (Fig. 2F-G). Based on ore and microprobe studies mineralogical paragenesis includes pyrite, chalcopyrite, magnetite, hematite and in some place galena (Fig. H-K).

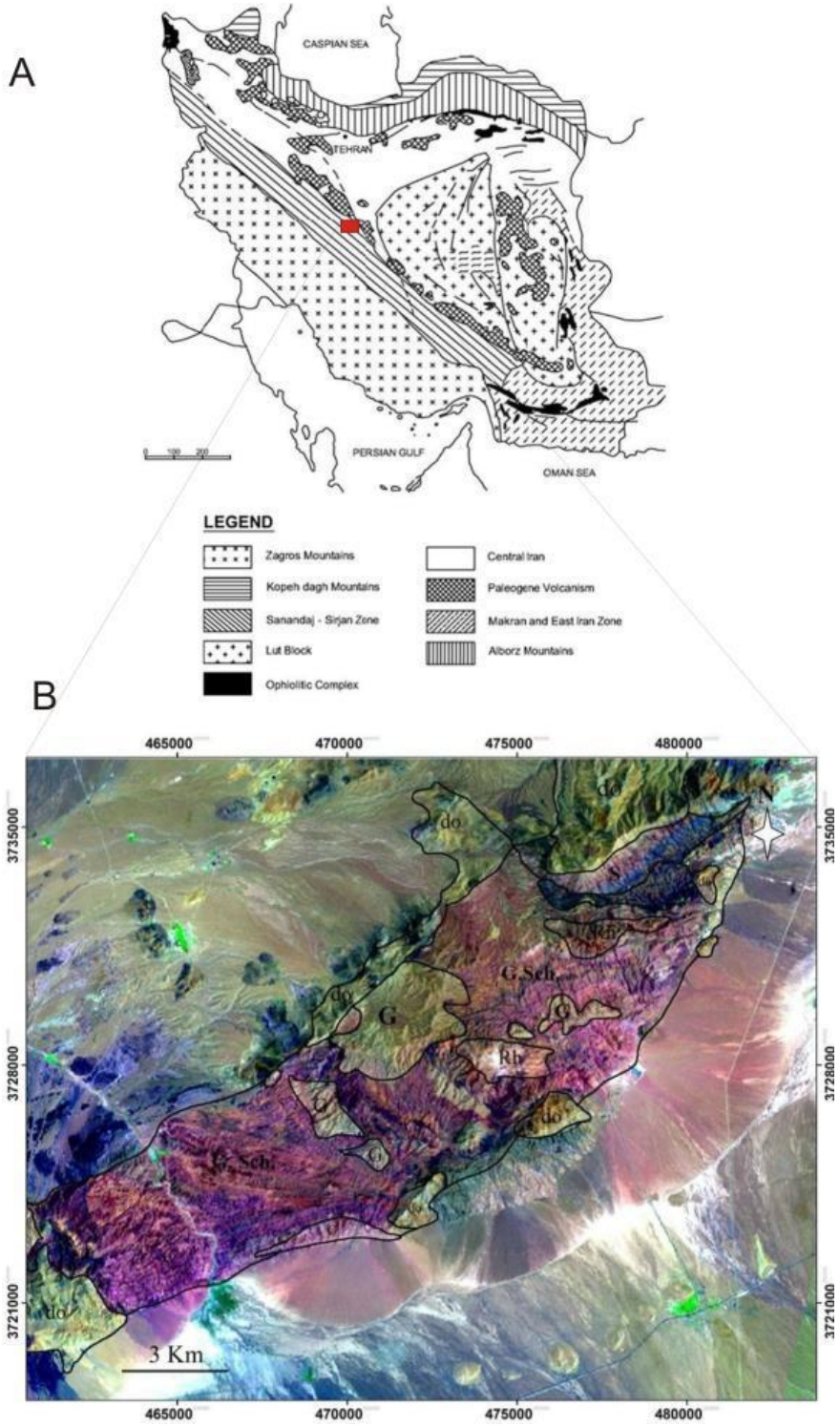

Fig. 1 a) Structural geology map of Iran, red rectangle indicates the location of study area, b) RGB Color composite Landsat ETM+ bands 7, 4 and 1, G:Granite, G.Sch: Green Schist complex, do: Dolomite, Rh:Rhyolite, S: Slate complex.

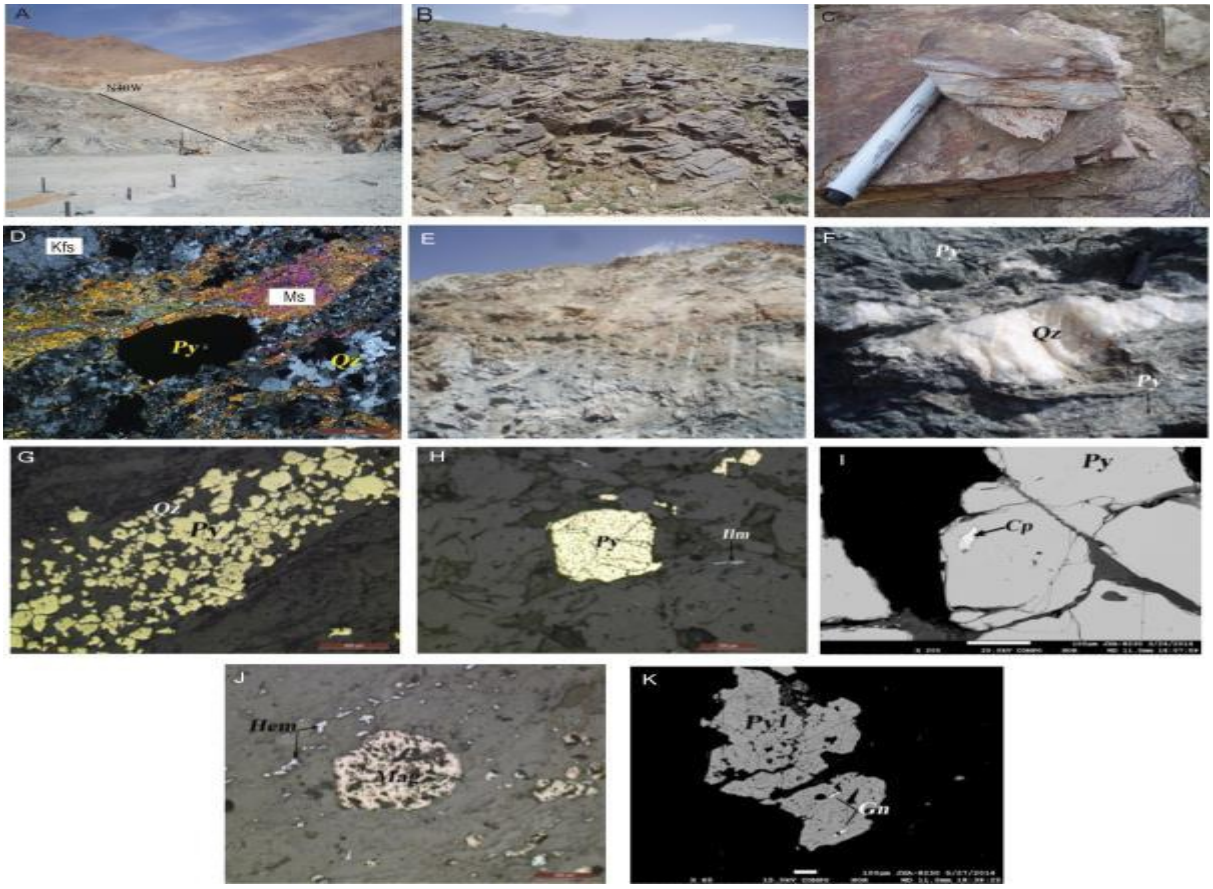

Fig. 2 a) The main fault of the senjedeh deposit , b) alteration of pyrite to iron oxides in surface parts, c) Hand specimen of felsic schist, d) photomicrograph of felsic schist (XPL), e) field photograph of argillic alteration, f) foliation in the ore-bearing quartz veins, g) pyrite in budding quartz veins, photomicrograph of h) pyrite and hematite, i) chalcopyrite, j) magnetite and hematite k) galena (Py=pyrite, Kfs=K-feldspar, Ms=Muscovite, Qz=Quartz, Hm= hematite, Cp= chalcopyrite, Mag= magnetite, Gn=galena)

3. Results and Discussion

It is assumed that pyrite is the main gold host in the Senjedeh deposit, although free gold or gold ores did not reveal during microscopic studies . In order to detect the abundance of gold and associated elements in pyrite (as the main gold-bearing mineral in this study), electron microprobe analysis (EPMA) analyzes were performed on 20 thin-polished and 4-polished sections. Based on microscopic observations, two generations of pyrite was identified:pyrite of first generation (G1) is characterized by anhedral to subhedral large grains along foliation, with high to medium gold content(0/bdl to 810ppm). Pyrite of second generation (G2) is characterized by euhedral grains with moderate to low gold content (0/bdl to 110ppm). In general, according to EPMA studies and BSE, gold is present in two types in a Senjedeh deposit, visible and invisible (according to Cook and Chryssoulis (1990) invisible gold including gold involved in the pyrite network and nanometer-sized particles and inclusions in pyrite): : Visible gold generally was observed among the mineral defects of pyrite with dimensions of less than 10 microns(Fig. 3A,B). It is noteworthy that these gold particles only exist within the deformed pyrite (G1), which could be attibute to the remobilization of invisible gold from minute inclusions in the pyrite during syn-deformational recrystallization (Cook et al., 2009). In general most of gold occur as nanometer-sized particles and inclusions in network pyrite (Fig. 3C), refrenced to invisible gold according to Cook et al (2009). . But it cannot be possible to ignore the presence of nano- particles gold involved in the pyrite network, because the presence of larger element than S such as As, Te, Sb (as it will follow in the next section) causes distortion of the pyrite crystal structure which facilitates incorporation of Au into pyrite (Cook et al.2009;Morishitaet al. 2018; Wan et al. 2018).

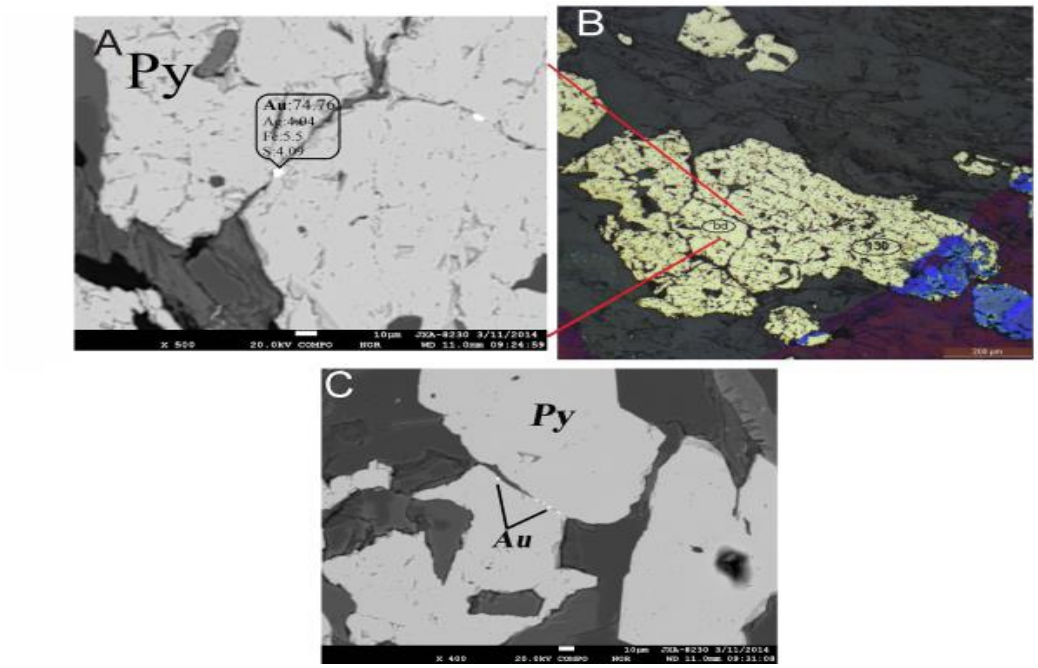

Fig. 3 a) Backscattered electron (BSE) images of pyrite (G1), b) Photomicrograph of Py(G1) in reflected light c) Backscattered electron (BSE) images of pyrite (G2)

3.1. Distribution of gold and trace elements in pyrite

Among the analyzed elements, the amount of iron and sulfide in pyrite are variable between 45/4 wt% to 46/9% wt% and 52/1wt% to 53/6 wt%, in respectively. Also the gold level is variable from 0/bdl (below the detection limit) up to 810ppm in the two generations of pyrite, first generation, being anhedral to subhedral, (G1) are oriented along foliation contain high to medium gold content (up to 810ppm), shows deformed and microfractured characteristic. The second generation of pyrite (G2) is euhedral with medium to low gold content(below limite of detection up to 110ppm). Except for gold, there is no systematic difference between the content of the trace elements in two generations of pyrite. It is noteworthy that As in both generations of pyrite is low and only in one sample reaches to 790 ppm, in most cases, it's value is variable from 0/bdl to the 790 ppm. The bivariate graphs of gold versus As, Te, Sb are plotted in Fig. 4. These diagrams Show that in the first and second generation pyrite (G1 and G2, respectively), no significant correlation was observed between gold and the three elements As, Te, Sb (Fig. 4 and Tab. 1) (except for the limited number in which the highest gold content (all with Au values above 0.4%wt) is associated with the lowest amount of Sb and even below the detection limit of the device for Sb)(Fig. 4).

Pearson correlation coefficient also suggests that the distribution of As, Te, Sb in the pyrite weakly correlates with Gold (0/024, -0/017, 0/031 respectively)(tab. 1),it could indicate the presence of gold as nanoparticles in the form of inclusions and along micro-fractures in the pyrite or at the grain boundary between pyrite minerals. The correlation coefficients between Bi and Au-Ag are among the highest in the Table, with Pearson coefficient values of 0.92 (Tab. 1). Arsenic does not correlate with gold and its concentration is low in the pyrite. The strong correlation between gold and silver indicates the occurrence of silver in gold deposit, the accompanying gold with Bi is common in gold deposits (Ciobanu et al. 2005). According to Cook et al (2013) strong correlation between Au and Ag- Bi is a sign of remobilization of these elements along gold. The researchers also explain why some of the Bi and Ag elements are mobile with gold but others, such as Te, Se, Co and Ni are not mobile. It might some elements be more locked inside the sulfide lattice, and therefore have a less tendency to mobility and some tend to be mobile (Cook et al. 2013).

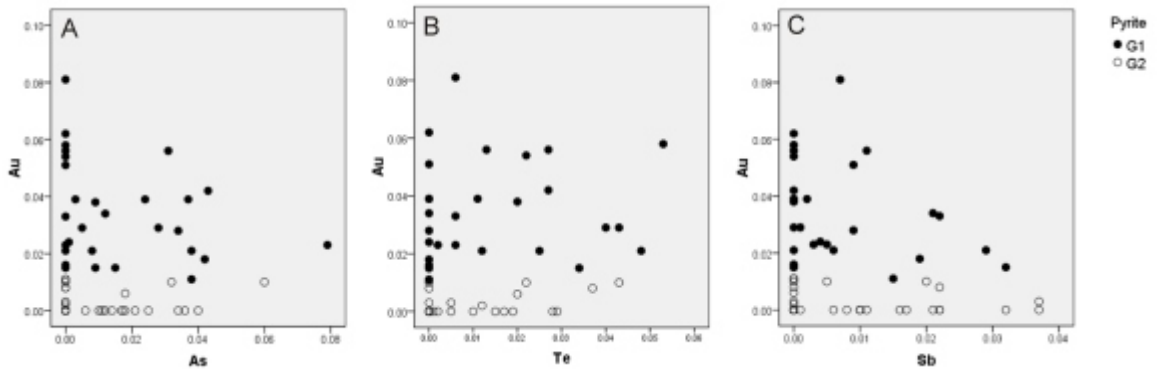

Fig. 4 Plots showing As, Te, Sb versus Au (see text).

Based on BSE images and EPMA analysis results, the first-generation subhedral and deformed pyrites have higher gold content than the second-generation euhedral pyrite. In BSE images visible free gold particles with diameters below 10 μm were observed in first-generation pyrite fractures, but in the second generation pyrite, no free gold was observed. The presence of gold particles along fractures in pyrite have been studied and reported by researchers such as Cook et al (2009), Large et al (2009) and Zhao et al (2011).The higher concentration of gold in fractured pyrite is possibly due to the accumulation of very fine gold inclusions (Zhao et al. 2011).

Since deformed pyrites are fractured and the fine gold particles is observed in these fractures (Fig. 3 A-C), it can be said that gold has been released from the pyrite network and accumulated in micro-fractures during metamorphic process. According to Cook et al. 2013, the movement of gold from the sulfide network and its re-focusing as inclusion or electrum between the parent minerals (arsenopyrite and pyrite), or at distance farther away, is known to be an important process for the enrichment in the gold deposits. This remobilization can be considered as an important process in orogenic gold deposits in which a sequence of fluid input and / or diffusion have taken place under temperature of green schist facies metamorphism or in principal stress directions. Morey et al (2008) by studying distribution of gold in pyrite and arsenopyrite in shear systems concluded that gold at the boundaries of these minerals could be as a result of mobility from previous pyrite and arsenopyrite, such process can also enrich the ore in the Senjedeh deposit. The EPMA data along with microscopic studies suggest that the distribution of gold in pyrite is strongly correlated with a post-mineralization process.

3.2. EPMA Mapping

In order to more precisely examine how gold and other elements occur in the pyrite, based on the results of the EPMA analysis, 5-crystals of pyrite mineral were selected to perform EPMA mapping(Fig. 5A-B). Based on these results, gold does not show any structural zoning (Fig. 5A-B), Only particles of gold are seen in the fractures, so much of the gold in pyrite exist in the form of nanoparticles rather than in the sulfide lattic. But the possibility of the presence of gold involved in the pyrite lattice cannot be ignored because the presence of large elements than S (such as As, Te, Sb) distort the pyrite network and allows gold to enter them and to be structurally bound in the crystal lattice as a sulfide-gold alloy (Cook et al.2009, Fougerouse et al, 2021). It could be said that Cu, Pb, Zn, Ag, Bi, Sb, Sn and W exist in pyrites in the form of mechanical mixtures of these elements, but most of the invisible gold contained in pyrite exist in the form of inclusions of nanoparticles. Since, these particles were found only in the microfractures of deformed pyrite (Fig. 3A-C), it can be inferred that the metamorphism causes the gold to be released from the pyrite network and to get accumulated in the microfractures.

Table 1. Pearson correlation coefficients of the EPMA trace element data for pyrite (G1)

	Se	As	S	Pb	Bi	Sb	Fe	Co	Ag	Te	Zn	Cu	Ni	Au
Se	1													
As	-0.025	1												
S	-0.109	0.058	1											
Pb	-0.047	0.027	0.039	1										
Bi	-0.054	0.074	-.598**	-0.006	1									
Sb	-0.057	-0.022	0.059	0.108	0.034	1								
Fe	-0.103	0.058	.997**	0.034	-.585**	0.062	1							
Co	-0.006	0.002	.192*	0.028	-0.054	-0.017	.174*	1						
Ag	-0.028	0.023	-.619**	-0.059	.920**	0.037	-.605**	-0.067	1					
Te	0.102	-0.03	0.065	-0.099	-0.009	-0.017	0.061	0.07	-0.019	1				
Zn	0.131	-0.058	-.385**	-0.106	0.112	-0.135	-.388**	-0.056	0.054	0.001	1			
Cu	.158*	-0.099	-.770**	0.001	0.01	-0.099	-.780**	-.181*	-0.023	-0.073	.444**	1		
Ni	-0.064	-0.049	0.037	-0.003	0.082	.160*	0.034	.289**	0.093	-0.038	-.184*	-0.117	1	
Au	-0.031	0.024	-.620**	-0.058	.920**	0.031	-.606**	-0.068	.969**	-0.017	0.056	-0.022	0.092	1

The trace elements in pyrite provide important information about the source of hydrothermal solutions and paleo-environmental conditions related to ore deposits. For example, high contents of Co, Ni, and Se indicate higher temperature, whereas high concentrations of As, Mo, Ag, Sb, Au, and Tl show the low temperature of pyrite formation (e.g., Sykora et al., 2018, Farhan et al., 2021). The lack of specific zoning in Au shows that gold in the pyrite of Senjedeh deposits is more likely to be free gold nanoparticles than involved in the pyrite network. Usually, Co is present in the pyrite network, which is sometimes accompanied by Ni. In this study cobalt is present almost in all samples and its concentration ranges between 130- 6030 ppm. It seems likely that the first-generation pyrites contain a cobalt-rich nucleus(Fig. 5B), but more studies (LA- ICP-MS mapping) are required to confirm. Other elements except Co show no specific zoning, of course, this zoning has lost its original order due to the deformation process. Ultramafic rocks and to a lesser extent mafic rocks are typically rich in Co, in contrast, felsic rocks usually contain its low levels (Farhan et al., 2021,). Highly differentiated magmatic rocks are usually rich in incompatible elements; therefore, pyrite associated with granite gold deposits is expected to have low Co. Therefore, high levels of cobalt in the pyrite in the region are a good indication of the presence of mafic and ultramafic rocks as a source of hydrothermal solutions compared to felsic and consistent with orogenic gold deposit.

A

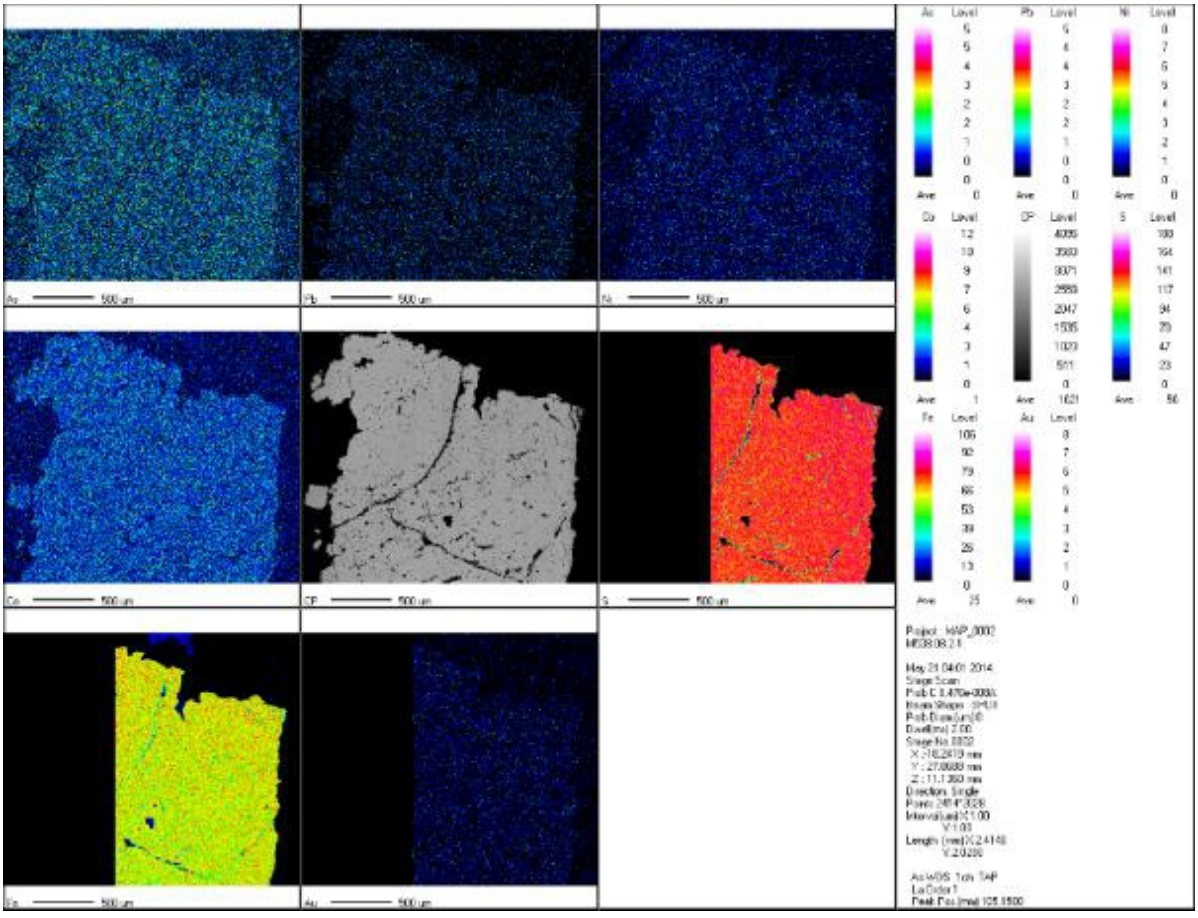

B

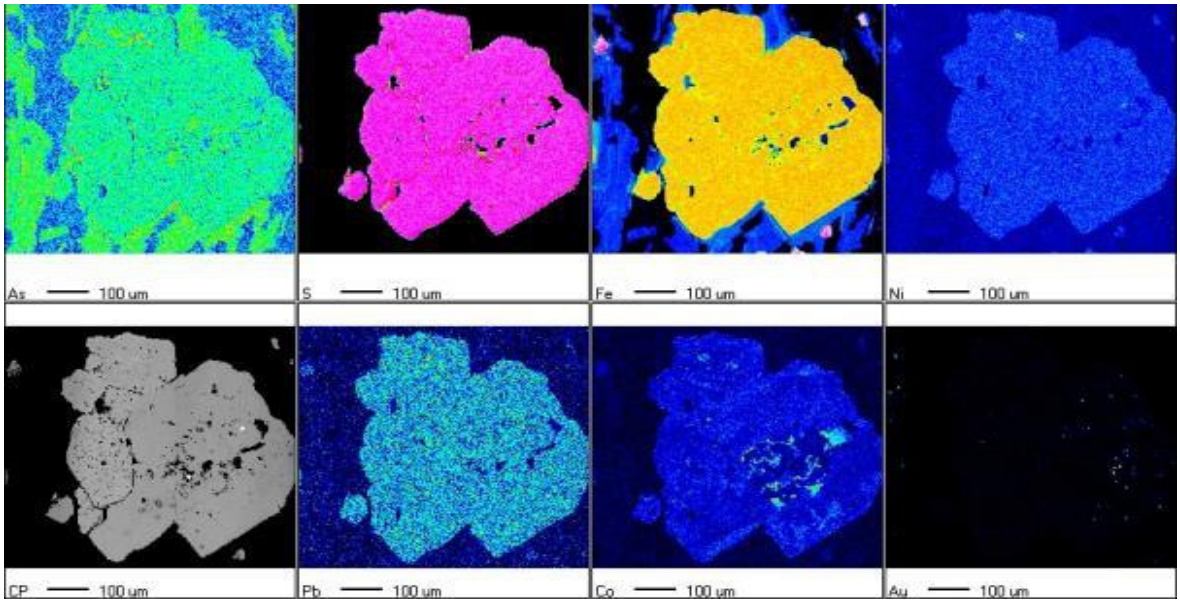

Fig. 5 a, b) EPMA mapping of pyrite in study area.

4. Conclusions

The gold mineralization in the study area occurred as quartz- sulfide veins and veinlets along N40W tending, NE dipping normal faults in metarhyolite host rock. Both macroscopic and microscopic scales quartz- sulfide veins and veinlets transect all metamorphosed and deformed country rocks. The most important hydrothermal alteration types are sericitization, kaolinitization, silicification and solfidization, where silica and sulfide alterations are developed in the inner parts of the fault zones adjacent to the mineralized zones. Mineralogical paragenesis includes magnetite, hematite, ilmenite, pyrite, chalcopyrite, galena, and gold. According to EPMA studies, gold is present in Senjedeh deposit as visible and invisible gold. Visible gold was found freely and generally less than 10 microns in the microtures of pyrite. According to this study, most of the gold in the Senjedeh deposit is invisible; this type of gold can also be involved in the pyrite network as well as the gold nanoparticles. Due to the presence of of elements such as As, Te, S, the pyrite network to be tilt and allow gold to enter the pyrite lattice, but most of the invisible gold in pyrite is in the form of inclusions of gold nanoparticles. In other hand, based on the results obtained from the EPMA mapping, gold does not show any compositional zoning, Only fine particles of gold can be seen freely. Therefore, gold in the pyrite of Senjedeh deposits is more likely to be free gold nanoparticles than involved in the network. The remarkable fact is these particles were found only in the microfractures of deformed pyrite. This indicates the importance of the metamorphic process in the mineralization of the region, so the metamorphism causes the gold to be released from the pyrite network and to get accumulated in the microfractures. Generally according to EPMA mapping, except for cobalt, there is no systematic difference between the content of the trace elements in two generations of pyrite. Cobalt-rich nucleus in the pyrite in the study area are a good indication of the presence of mafic and ultramafic rocks and consistent with orogenic gold deposit

Acknowledgements

The authors acknowledge the support of Shahid Beheshti University and Iran Minerals Production and Supply Company (IMPASCO) in the completion of this research. The authors also would like to thanks Chinese Academy of Geological science for providing the necessary facilities to carry out this research. The authors declare that they have no conflict of interest.

Authors' Contribution

Zahra Nourian Ramsheh and Mohammd Yazdi, proposed the main concept and involved in write up. Seyedeh Narges Sadati, assisted in analyzing data and in preparation of

illustration and plates of figures. Fariborz Masoudi, collected field data. Jingwen Mao, did provision of relevant literature, and review and proof read of the manuscript, also he funded the analysis in his laboratory.

References

Agangi, A, Przybyłowicz, W. Hofmann, A., 2015. Trace element mapping of pyrite from Archean gold deposits – A comparison between PIXE and EPMA, Nuclear Instruments and Methods in Physics Research Section. Beam Interactions with Materials and Atoms 348, 302-306.

Alavi, M. 2004., Tectonics of the Zagros orogenic belt of Iran: new data and interpretation. Tectonophysics, 229, 211-238.Alavi, M. 2004., Regional stratigraphy of the Zagros fold-thrust belt of Iran and its proforeland evolution. American Journal of Science, 304, 1–20.

Alipour-Asll, M. 2018., Geochemistry, fluid inclusions and sulfur isotopes of the Govin epithermal Cu-Au mineralization, Kerman province, SE Iran. Gexplo, 196, 156-172.

Aliyari, F. Rastad, E. Mohajel, M. 2012., Gold Deposits in the Sanandaj–Sirjan Zone: Orogenic Gold Deposits or Intrusion-Related Gold Systems. Resource Geology 62, 296–315.

Almasi, A. Yousefi, M. Carranza, E.J.M. 2017., Prospectivity analysis of orogenic gold deposits in Saqez-Sardasht Goldfield, Zagros Orogen, Iran. Ore Geology Reviews 91, 1066-1080.

Amponsah, P. Salvi, S. Didier, B. Baratoux, L. Siebenaller, L. Jessell, M. Mackenzie Nude, P. Gyawub, E A. 2016., Multistage gold mineralization in the Wa-Lawra greenstone belt, NW Ghana: The Bepkong deposit. Journal of African Earth Sciences 120, 220-237.

Cook N., Coibanu, C., Mao, J., 2009, Textural control on gold distribution in As-free pyrite from the Dongping, Huangtuliang and Hougou gold deposits, North China Craton (Hebei Province, China), Chemical Geology 264(1), 101-121

Farhan, M., Arif, M., Ying, Y.,Chen, X., Garbe-Schönberg, G., Li, C., Hussain, Z., Ullah, Z., Zhang, P., Khan, A., Fluid source, element mobility and physicochemical conditions of porphyry-style hydrothermal alteration-mineralization at Mirkhani, Southern Chitral, Pakistan, Ore Geology Reviews, 135, doi.org/10.1016/j.oregeorev.2021.104222.

Fougerouse, D., Reddy, S., Aylmore, M., Yang, L., Guagliardo, P.,; Saxey, D., Rickard, W.,Timms, N., 2021, A new kind of invisible gold in pyrite hosted in deformation-related dislocations, Geology, doi.org/10.1130/G49028.1.

Li, Z. Zhu, X. Lu, H. Han, T. 2013., The occurrence of gold in pyrite from the Liulincha gold ore belt, western Hunan Province, China. China Journal Geochemistary 32,392–397.

Masoudy, f., 1997. Contact metamorphism and pegmatite development in the region SW of Arak, Iran, Ph.D. thesis, university of leeds, Uk.

Mohajjel, M. Fergusson, C L. Sahand, MR. 2003., Cretaceous-Tertiary convergence and continental collision, Sanandaj-Sirjan zone, western Iran. Journal of Asian Earth Sciences 21, 397-412.

Morishita, Y. Shimada, N. Shimada, K. 2018., Invisible gold in arsenian pyrite from the high-grade Hishikari gold deposit, Japan: Significance of variation and distribution of Au/As ratios in pyrite. Ore Geology Reviews 95, 79-93.

Steven, M. Robert, R,.Hough, M. 2013., Microstructural evolution and trace element mobility in Witwatersrand pyrite. Contrib Mineral Petrol 166, 1269–1284.

Wan, B. Yang, W. Deng, C. Xiao, C. 2018., Rb-Sr geochronology of single gold-bearing pyrite grains from the Katbasu gold deposit in the South Tianshan, China and its geological significance. Ore Geology Reviews 100, 99-110.